tributaries suggested that these features "could" be warm-based (Joughin and others, 1999). Our observation is evidence in support of this suggestion.

Subglacial lakes are likely to contain water and sediment at a ratio that is unknown. It is therefore possible that some subglacial lakes, especially those noted as "possible" lakes by Siegert and others (1996), are in fact pockets of water-saturated sediments. This, however, does not affect the implications of our observation, since it is indisputable that both subglacial lakes and water-saturated sediment pockets are evidence of liquid-water storage. We note that some ice streams have no subglacial lakes yet identified beneath their upstream tributaries. There are several explanations for the apparent absence of lakes in such areas. First, several enhanced ice-flow features have yet to be surveyed by airborne radar. Second, radar data from no more than a few flight-lines are available for any of the flow features, and it is highly possible that the existing lines missed relatively small lakes. Third, subglacial lakes are only able to build up where there are topographic hollows. In the absence of such topography, lakes are not able to form despite the presence of subglacial water. Fourth, subglacial-lake detection by radar methods is not possible if the ice base is "fluted" due to sliding-induced erosion, because radar energy is "scattered" by rough surfaces. Because of this, there may be only a narrow region of the ice sheet, between the enhanced-flow feature and the frozen ice-sheet base, where subglacial lakes can be detected. These explanations lead us to think that the presence of subglacial lakes in some onset regions of enhanced ice flow suggests there is likely to be subglacial water in other glaciologically similar regions.

Several subglacial lakes thought previously to be located in the slow-moving central region of the ice sheet are, in fact, at the margins of enhanced ice flow. Subglacial lakes near to South Pole are adjacent to an outlet glacier system deep within the Antarctic continent that flows into the Filchner–Ronne Ice Shelf. This indicates that warm-based flow of ice (i.e. basal sliding and/or deformation of subglacial sediment) can initiate near the centre of the ice sheet, and extend continuously between this region and the margin of the ice sheet where ice streams terminate. Unless the ice-sheet base becomes frozen downstream of these lakes, which is improbable given the steady increase in ice flux calculated along these flow features, there should be a subglacial hydrological connection between the onset regions of enhanced flow, where our lakes are located, and the ice streams further downstream. Because of this, several enhanced-flow features that initiate in the inner Antarctic ice sheet can be thought of as being warm-based across their entire length. The identification of warm-based ice-sheet outlets is of value as a boundary condition to those building numerical models of the Antarctic ice sheet, since the subglacial thermal regime is critical to the flow of ice.

We note that lack of radar data in some regions means that our observation of subglacial lakes at the head of enhanced ice-flow features is not comprehensive. However, we hope that our finding will encourage other glaciologists to acknowledge the possibility of stored water at these locations, and accept that the ice sheet is warm-based along several relatively long ice-sheet outlets.

ACKNOWLEDGEMENTS

We thank R. Bindschadler for a constructive and helpful review, and M. Sturm for editorial guidance. Funding for this work was provided by U.K. Natural Environment Research Council grants GR9/4782 to M.J.S. and GR3/9791 to J.L.B.

Bristol Glaciology Centre,
School of Geographical Sciences,
University of Bristol,
Bristol BS8 1SS, England

MARTIN J. SIEGERT
JONATHAN L. BAMBER

6 September 2000

REFERENCES

Bamber, J. L. and R. A. Bindschadler. 1997. An improved elevation dataset for climate and ice-sheet modelling: validation with satellite imagery, *Ann. Glaciol.*, **25**, 439–444.

Bamber, J. L., D. G. Vaughan and I. Joughin. 2000. Widespread complex flow in the interior of the Antarctic ice sheet. *Science*, **287**(5456), 1248–1250.

Budd, W. F. and R. .C. Warner. 1996. A computer scheme for rapid calculations of balance-flux distributions. *Ann. Glaciol.*, **23**, 21–27.

Dowdeswell, J. A. and M. J. Siegert. 1999. The dimensions and topographic setting of Antarctic subglacial lakes and implications for large-scale water storage beneath continental ice sheets. *Geol. Soc. Am. Bull.*, **111**, 254–263.

Dowdeswell, J. A. and M. J. Siegert. In press. The physiography of modern Antarctic subglacial lakes. *In* Fard, A. M., *ed. Subglacial lakes: a planetary perspective.* Boulder, CO, Geological Society of America. (GSA Special Paper.)

Joughin, I. *and 7 others.* 1999. Tributaries of West Antarctic ice streams revealed by RADARSAT interferometry. *Science*, **286**(5438), 283–286.

Siegert, M. J., J. A. Dowdeswell, M. R. Gorman and N. F. McIntyre. 1996. An inventory of Antarctic sub-glacial lakes: *Antarct. Sci.*, **8**(3), 281–286.

Vaughan, D. G., J. L. Bamber, M. B. Giovinetto, J. Russell and A. P. R. Cooper. 1999. Reassessment of net surface mass balance in Antarctica: *J. Climate*, **12**(4), 933–946.

SIR,

The chemistry of grain boundaries in Greenland ice

The spatial variation of impurities found in natural polycrystalline ice has been of interest for over a century. Based on thermodynamic arguments, Harrison and Raymond (1976) suggested that impurities in temperate glacier ice reside to varying degrees in three-grain intersections or triple junctions (TJs). Thus far, however, there have been only two studies of the microchemistry of natural ice. In the first study, Wolff and co-workers (Mulvaney and others, 1988; Wolff and others, 1988) showed, using X-ray microanalysis in a scanning electron microscope (SEM), that the TJs contained substantial concentrations of sulfate ions. The ice, obtained from Dolleman Island, Antarctica, was coated with aluminum and held at a temperature of −160°C during analysis. Neither S nor Cl were detected elsewhere in the ice. Later, Fukazawa and others (1998) used micro-Raman spectroscopy to study ice from two Antarctic sites. At temperatures between −8° and −35°C in Nansen ice, NO_3^- and HSO_4^- were found as liquids at the TJs, while at temperatures between −8° and −20°C in South Yamato ice, SO_4^{2-} was found as a liquid at the TJs.

The ice studied here was from an ice core (specimen depth 214 m) at the Greenland Ice Sheet Project II (GISP2) site. It was stored at −20°C at the National Ice Core Laboratory, Boulder, Colorado, U.S.A., before examination at Dartmouth. Specimens with dimensions of ~25 mm × 25 mm by 10 mm thick were cut from the ice, and the surface carefully shaved

https://doi.org/10.3189/S0022143000212756 Published online by Cambridge University Press

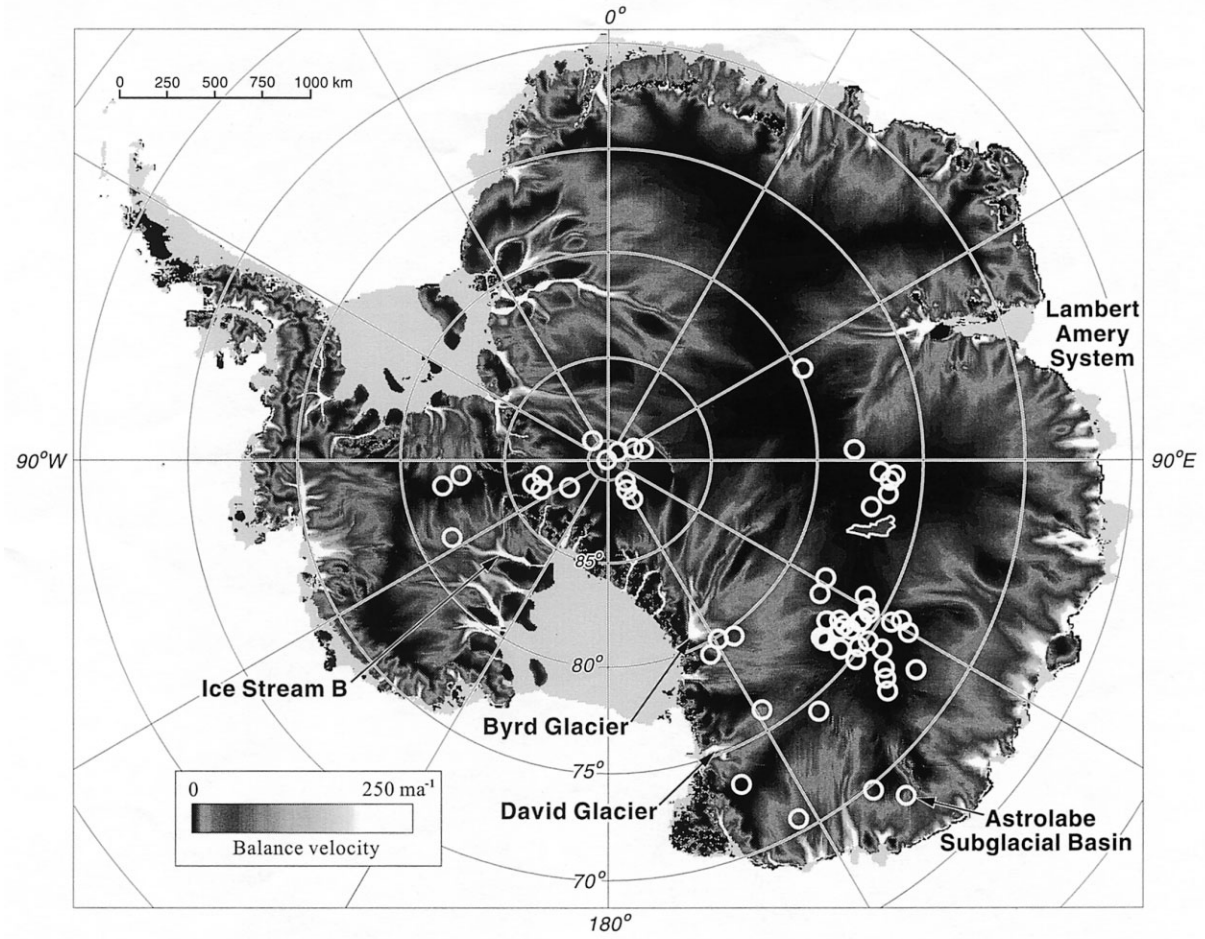

Fig. 1. Three GBs meet at a TJ (2) in ice which has been allowed to sublimate for 8 weeks. Note the filament lying along the upper left GB (1), and the smaller filament at the right of the horizontal GB (A). 3 is a white spot in the grain interior. The inset is a reduced version of the figure in which the lines indicate the GB channels.

with a razor blade in a high-efficiency particle-air- filtered, laminar-flow hood following standard clean-room practices. The specimens were examined using a JEOL 5310LV low-vacuum SEM, equipped with a PGT IMIX energy-dispersive X-ray microanalysis system (EDS) utilizing a pure germanium, thin-window detector. The SEM was operated at 10 kV and utilized a cold stage cooled to -115 ± 5°C. Four SEM images, and associated EDS data (normalized to 100 000 total counts), are shown here from uncoated GISP2 ice. The elements indicated on the X-ray spectra are the impurities typically found in glacier ice (Mayewski and others, 1993). Nitrogen, which is present in both NO_3^- and NH_4^+, is not indicated since it was not found in any specimen. EDS data were collected from a number of different regions in the ice: TJs, grain boundaries (GBs), grain interiors, "filaments" and inclusions were all analyzed.

Figure 1 shows the ice after it was allowed to sublimate in a small sealed container for 8 weeks at −20°C. The large GB channels (see inset) are typical of the long sublimation time. Sublimation preferentially occurs at the GBs because these are regions of high energy. Sublimation also led to grain faceting, a feature previously noted by Cross (1969). At the upper left is a ~1.0 μm diameter filament in the center of a GB channel (labeled 1). EDS data from the filament (Fig. 2a) showed that it is composed chiefly of Cl, Mg and Na, although small S (from SO_4^{2-}) and Ca peaks are also present. Filaments were observed along many GBs, and all contained large amounts of Cl and Na, while the occurrence of the other common glacier impurities appears to be happenstance. Note that in Figure 1 filaments were absent along the other two GBs, although a smaller filament fragment is present in the horizontal GB (labeled A). Filaments appear to be attached relatively loosely to the ice and move around readily, particularly when the electron beam is focused on them or when the specimen is undergoing rapid cool-down. EDS of the small white spot located within the TJ center (labeled 2) showed predominantly Cl and Na (Cl is less than in the filament), with a minute S peak, while EDS of the white spot in the grain interior (labeled 3) showed low impurity levels, with minute S, Cl and Na peaks, typical of spectra from other white points within grains.

To study the effect of a short sublimation time, the specimen in Figure 1 was reshaved with a razor and then allowed to sublimate in a sealed container at −20°C for 2 hours. The GB channels (Fig. 3) are not present, indicating minimal sublimation, but the GBs are easily distinguished by the small white impurity spots and the different sublimation patterns of the grains (which depend on their crystallographic orientation). The inset in Figure 3 is a higher magnification image of an inclusion and a filament from the GB adjacent to the lower TJ. EDS data (Fig. 2b) showed that the inclusion (labeled 4) consisted of S, Cl, Na, Ca and a small amount of Mg, while the filament (labeled 5) and the white spot on the GB labeled 6 contained only Cl and Na.

The formation of the GB filaments is thought to occur as a result of preferential sublimation of pure ice, which surrounds the impurities that have segregated to the GB. The examination temperature was well below the eutectic temperature of

https://doi.org/10.3189/S0022143000212756 Published online by Cambridge University Press

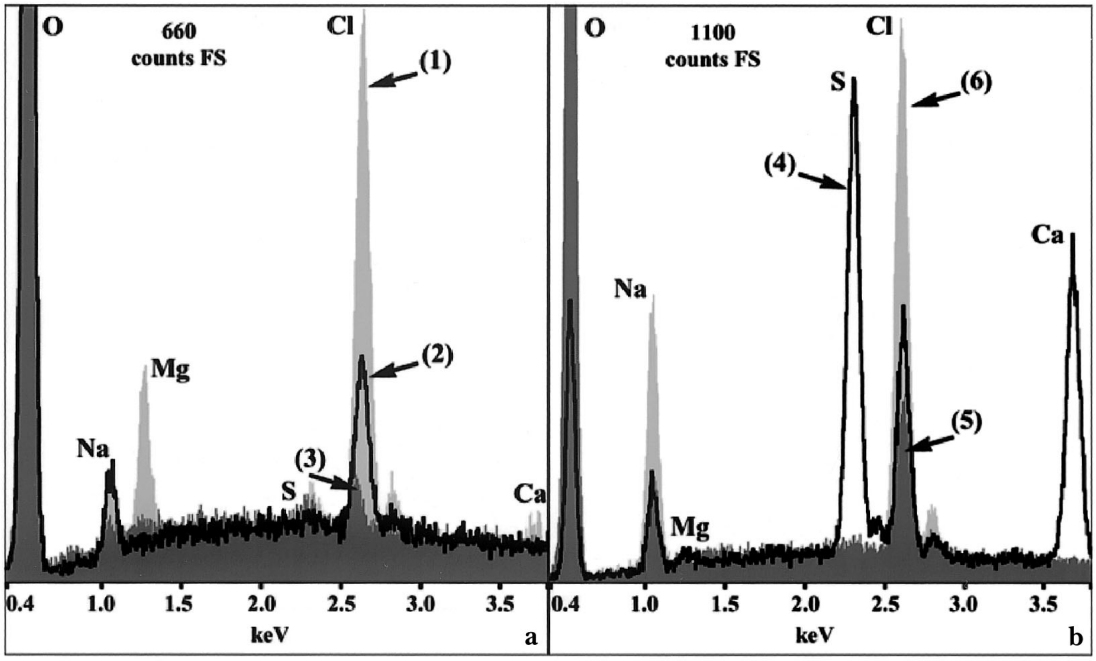

Fig. 2. (a) EDS spectra from the points indicated in Figure 1: (1) GB filament; (2) TJ white spot; (3) white spot in grain interior. (b) EDS spectra from the points indicated in Figure 3: (4) spherical inclusion near TJ; (5) filament adjacent to inclusion; (6) GB white spot. The ordinate axis indicates X-ray counts, and the abscissa indicates the energy; the relative concentration of each element is given by the area under the peak. The peak on the far left is oxygen from the ice and/or hydrated impurities; the small unlabeled peaks sometimes present to the right of the S or Cl peaks are the K_β peaks for these elements.

any of the H_2O-impurity systems for the observed impurities, so it is possible that the filaments are hydrated salts which coalesced (to reduce surface energy) after the surrounding ice sublimated. An estimate can be made of the expected filament diameter by assuming that a sheet of impurities 1 nm thick resided at the GB, and that the depth of the GB channel in Figure 1 is half its width of 250 μm. The resulting cylindrical filament would have a diameter of 0.4 μm that is comparable

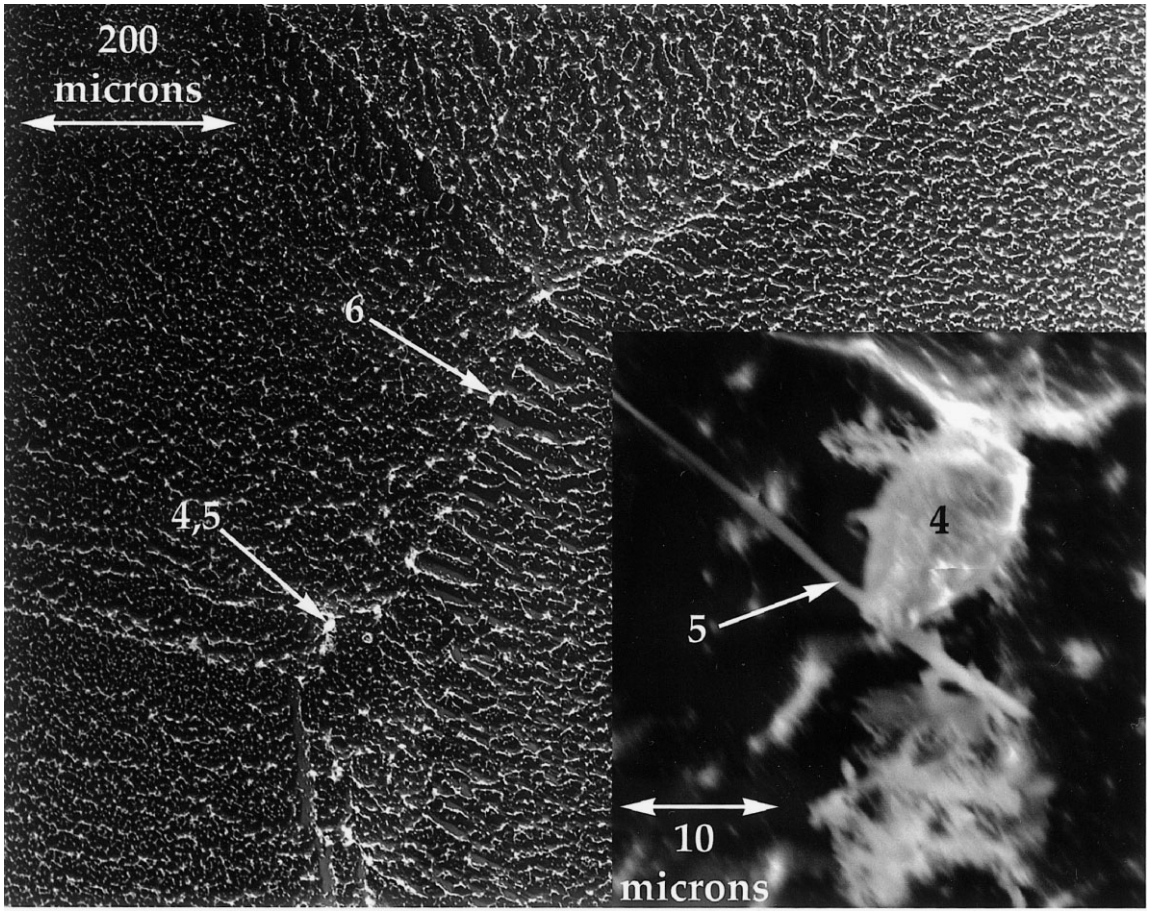

Fig. 3. Two TJs and connecting a GB in ice. Inset: Spherical inclusion and filament from GB area near the lower TJ. The specimen had been allowed to sublimate for 2 hours.

https://doi.org/10.3189/S0022143000212756 Published online by Cambridge University Press

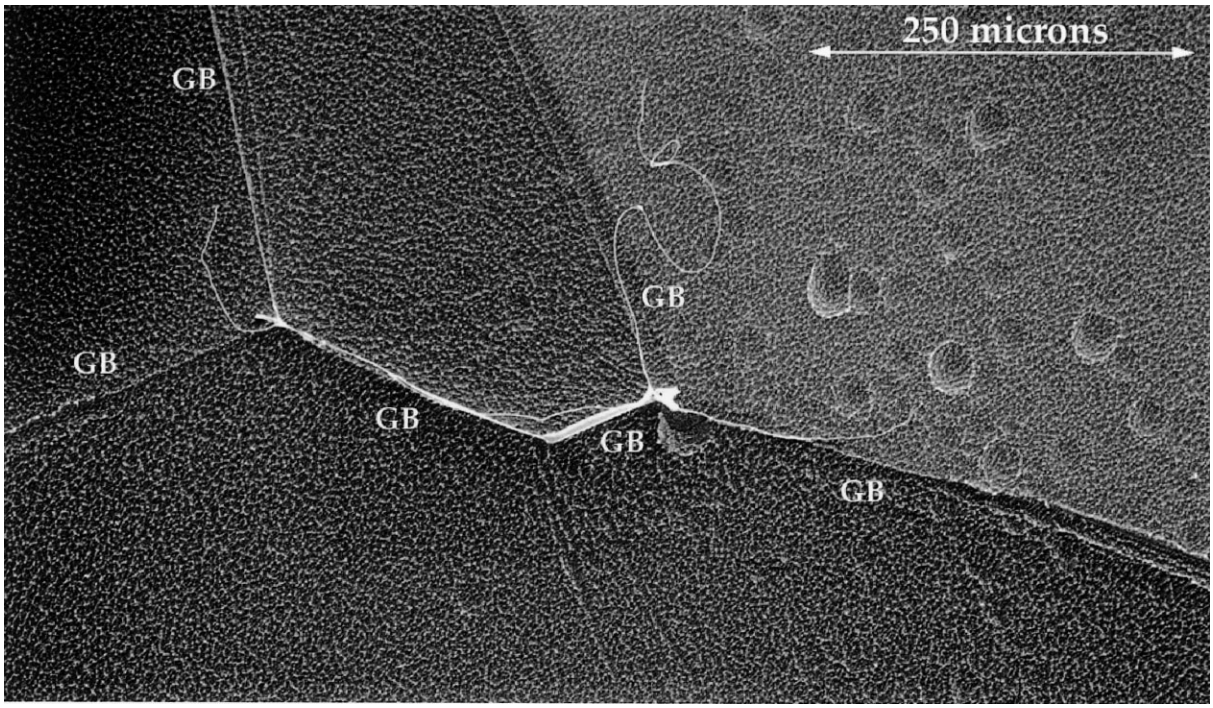

Fig. 4. Image of ice showing GB filaments. Note that some of the filaments have peeled out of the GB.

to the observed ~1 μm filament width in Figure 1. Similarly, coalescence of impurities, via surface diffusion, could explain the formation of the white impurity spots in the grain interiors. It is worth noting that the longer a specimen sublimates, the more numerous and larger become the white spots on both the grain interiors and the GBs, and the more likely the spots are to contain detectable levels of impurities. No detectable impurities were found in the dark areas of any specimen.

Any doubt that the filaments observed in the previous images originated from the GB should be alleviated by Figure 4 in which the association between the filaments and the GB region is clearly illustrated along with the transient nature of the filaments. The thinner filament sections are peeling away from the GB channels, the impetus for this movement probably being the rapid cool-down of the specimen and the large difference in the thermal expansion coefficient of NaCl (~28 $°C^{-1}$ at −120°C) and ice (~90 $°C^{-1}$ at −120°C).

Wolff and co-workers stated that between 40% and quite possibly all of the H_2SO_4 in the Dolleman Island ice they studied was at the TJs. They suggested that if this result could be generalized to all Antarctic and polar ice it could explain the d.c. conductivity of the ice. Our results, showing high concentrations of S in inclusions (Fig. 2b), trace amounts in the grain interiors, but only small amounts at the TJs, suggest that all the H_2SO_4 is not located in TJs in polar ice. This observation was indirectly confirmed by Fukazawa and others (1998), who estimated that $<3\%$ of the H_2SO_4 in their South Yamato ice was at the TJs. On the other hand, Wolff and co-workers proposed (but did not observe, since they did not find any Cl) that it is thermodynamically preferable for NaCl in polar ice to form "pure volumes" of NaCl which would eventually partition to the GB. Our data (small Cl concentrations in the grain interiors, but large concentrations in the form of filaments in the GB) would seem to confirm this suggestion. It should be noted that the GISP2 site is located in the opposite hemisphere, is colder and is farther from the ocean, and that the specimens studied here were obtained from different depths than the sites from which Wolff and co-workers or Fukazawa and others (1998) obtained their ice. Therefore, a direct comparison between their data and ours is not possible.

In summary, filaments composed mostly of NaCl were observed in GBs of ice from GISP2. The filaments appear to be the result of preferential sublimation of ice at the GBs leaving behind the impurities. In addition, small amounts of impurities (mainly S and Cl^-) were found in the grain interiors, while large concentrations of S were observed in inclusions.

ACKNOWLEDGEMENTS

This research was supported by grants from the U.S. National Science Foundation (OPP-9980379) and the U.S. Army Research Office (DAAD 19-00-1-0444).

Thayer School of Engineering,
Dartmouth College,
Hanover,
New Hampshire 03755-8000,
U.S.A.

D. Cullen
I. Baker

21 September 2000

REFERENCES

Cross, J. D. 1969. Scanning electron microscopy of evaporating ice. *Science*, **164**(3876), 174–175.

Fukazawa, H., K. Sugiyama, S. Mae, H. Narita and T. Hondoh. 1998. Acid ions at triple junction of Antarctic ice observed by Raman scattering. *Geophys. Res. Lett.*, **25**(15), 2845–2848.

Harrison, W. D. and C. F. Raymond. 1976. Impurities and their distribution in temperate glacier ice. *J. Glaciol.*, **16**(74), 173–181.

Mayewski, P. A. *and 7 others*. 1993. The atmosphere during the Younger Dryas. *Science*, **261**(5118), 195–197.

Mulvaney, R., E. W. Wolff and K. Oates. 1988. Sulphuric acid at grain boundaries in Antarctic ice. *Nature*, **331**(6153), 247–249.

Wolff, E. W., R. Mulvaney and K. Oates. 1988. The location of impurities in Antarctic ice. *Ann. Glaciol.*, **11**, 194–197.